Review article

Bin Liang*, Jian-chun Cheng and Cheng-Wei Qiu

Wavefront manipulation by acoustic metasurfaces: from physics and applications

https://doi.org/10.1515/nanoph-2017-0122
Received December 6, 2017; accepted January 21, 2018

Abstract: Molding the wavefront of acoustic waves into the desired shape is of paramount significance in acoustics, which however are usually constrained by the acoustical response of naturally available materials. The emergence of acoustic metamaterials built by assembling artificial subwavelength elements provides distinct response to acoustic waves unattainable in nature. More recently, acoustic metasurfaces, a class of metamaterials with a reduced dimensionality, empower new physics and lead to extended functionalities different from their three-dimensional counterparts, enabling controlling, transmitted or reflected acoustic waves in ways that were not possible before. In this review paper, we present a comprehensive view of this rapidly growing research field by introducing the basic concepts of acoustic metasurfaces and the recent developments that have occurred over the past few years. We review the interesting properties of acoustic metasurfaces and their important functionalities of wavefront manipulation, followed by an outlook for promising future directions and potential practical applications.

Keywords: acoustics; metasurfaces; wavefront manipulation; diffusers; energy absorption.

***Corresponding author: Bin Liang,** Collaborative Innovation Center of Advanced Microstructures and Key Laboratory of Modern Acoustics, MOE, Institute of Acoustics, Department of Physics, Nanjing University, Nanjing 210093, P.R. China, e-mail: liangbin@nju.edu.cn
Jian-chun Cheng: Collaborative Innovation Center of Advanced Microstructures and Key Laboratory of Modern Acoustics, MOE, Institute of Acoustics, Department of Physics, Nanjing University, Nanjing 210093, P.R. China
Cheng-Wei Qiu: Department of Electrical and Computer Engineering, National University of Singapore, 4 Engineering Drive 3, Singapore 117583, Singapore

1 Introduction

How to manipulate the wavefront of acoustic waves simply and efficiently is a key problem in acoustics and also the subject of many diverse areas. As representative examples, in high-intensity focused ultrasound therapy the acoustic energy must be converged into the target focal region with high precision for heating the tumor; in loudspeaker design or underwater communications various acoustic beams with special directivity need to be formed for delivering acoustic signals to far field. Due to the limitation in the acoustical properties provided by naturally available materials, however, wavefront engineering is still challenging and generally has to rely on fabricating materials of given refractive indexes into intricate shapes or using a large array of individually controlled active elements, such as the piezoelectric transducers with curved profile for producing high-intensity focused ultrasound or the large-sized array of sensors for underwater applications. In addition, control of acoustic waves of long wavelength with a compact device would be highly desirable in a great variety of important situations such as noise cancellation, yet is extremely difficult for existing technologies since classic theory of acoustics usually requires the device size and the wavelength to be comparable for giving rise to effective wave-structure interaction. This is evidenced by lots of everyday phenomena such as the sound absorptive wedges with large length used in anechoic chamber and the acoustic barriers that need to be bulky for shielding low-frequency sound and so on.

In the past two decades, considerable attention has been dedicated to metamaterials which first appeared in the field of electromagnetics [1–4] and were then extended to acoustics [5–8]. Metamaterials are artificial composite structures built by assembling a set of resonant elements, with each being much smaller than the working wavelength and regarded as an artificial "atom" (or meta-atom), throughout a region of space. Due to the subwavelength scale of an individual meta-atom, the inhomogeneity of the array formed by them cannot be "seen" by the acoustic wave. As a result, these meta-atoms, in the bulk, behave like a continuous medium with unconventional acoustic bulk properties [9, 10]. By engineering the subwavelength microstructure of meta-atoms, it is possible to achieve effective acoustical parameters (viz., effective mass density and effective bulk modulus) unattained with natural materials, e.g. single or double negative parameters [5–8, 11], near-zero parameters [12–14], and extremely anisotropic parameters [15–20] for acoustic waves. With such extraordinary acoustic responses, acoustic metamaterials enable acoustic wavefront manipulation at subwavelength scales and may lead to novel artificial bulk devices capable to produce many fascinating phenomena, including acoustic superlens and hyperlens for achieving resolution beyond the diffraction limits inherent in conventional lenses [21, 22], cloaks for making objects acoustically "invisible" by cancelling the scattered waves on its surface as impinged by acoustic waves [23–26] or for creating acoustic "illusions" by changing the spatial pattern of scattered field [27, 28].

In this context, a question seems to be natural: is it possible to freely modulate the wavefront of acoustic wave as it transmits through or is reflected by an interface between two media? It is expectable that such functionality of wavefront steering with a reduced dimension, if realized, would not only enable wave physics innately different from three-dimensional metamaterial systems but open doors to the design of novel functional devices with small footprint, planar profile, and low loss and promote their applications in various important scenarios. Unfortunately, from the viewpoint of classic acoustics, the answer should be NO. It is well known that the reflection and refraction of acoustic waves is always governed by Snell's law, which tells that the reflection and incidence angles are exactly equivalent and the ratio between the refraction angle and incident angle depends on the ratio between the refractive indexes of the two media, as we have long believed.

2 Generalized Snell's law and metasurface

In 2011, Yu et al. [29] have proven, both theoretically and experimentally, that by introducing abrupt phase shift as light traverses the interface between two media, we can revisit the classic law of reflection and refraction and attain a new degree of freedom for controlling the wavefront. By designing a constant phase gradient along the interface, referred to as $\mathrm{d}\Phi/\mathrm{d}x$, one can derive the generalized Snell's law from the Fermat's principle for the incident wave at an angle θ_i, as follows

$$n_\mathrm{t}\sin(\theta_\mathrm{t})-n_\mathrm{i}\sin(\theta_\mathrm{i})=\frac{\lambda_0}{2\pi}\frac{\mathrm{d}\Phi}{\mathrm{d}x},\ \sin(\theta_\mathrm{r})-\sin(\theta_\mathrm{i})=\frac{\lambda_0}{2\pi n_\mathrm{i}}\frac{\mathrm{d}\Phi}{\mathrm{d}x}, \tag{1}$$

where θ_t and θ_r are the angles of refraction and reflection, n_i and n_t are the refractive indexes of the two media at the incident and transmission sides, respectively, and λ_0 is the free-space wavelength.

Such phase discontinuities were imprinted on propagating light experimentally by using a two-dimensional array of optical resonators, denoted as "metasurface" for light, which modifies the boundary condition by the resonant excitation of antenna current. The generalized Snell's law implies the possibility of arbitrarily manipulating the directions of reflected and refracted waves by modulating the phase gradient along the metasurface, which is achievable via adjustment of structural parameters of resonators. If there is no spatial gradient of propagation phase along the interface, Eq. (1) degenerates to the conventional Snell's law. It is noteworthy that metasurfaces are not necessarily of zero thickness; the constituent resonators composing metasurfaces can have arbitrary shapes and a dimension required to be small only in terms of the working wavelength [30].

Despite the great potential possessed by the generalized Snell's law for light, the design of optical metasurfaces cannot be directly transplanted into acoustics, considering the inherent distinction between acoustic and electromagnetic waves. Optical metasurfaces have to be implemented by exploiting the plasmonic resonance that has no direct counterpart in acoustics so far [31–33]. In addition, the mechanism for designing optical metasurfaces makes it difficult to shrink the thickness of resulting devices down to deep-subwavelength scale. Therefore, the realization of acoustic metasurfaces can be expected to have deep implication in the whole field of acoustics but needs to be based on the exploration of new mechanisms.

3 Reflective-type acoustic metasurfaces

Considering the scalar nature of acoustic waves, they can propagate freely in a waveguide with subwavelength cross-section in the absence of cut-off frequency. Figure 1A shows the schematic of a unit cell of space-coiling type metamaterial with a width of a. In free space, the propagation distance of acoustic wave between points A and B is simply a. But in the presence of the labyrinthine-like structure formed by coiling up space [35, 36], the

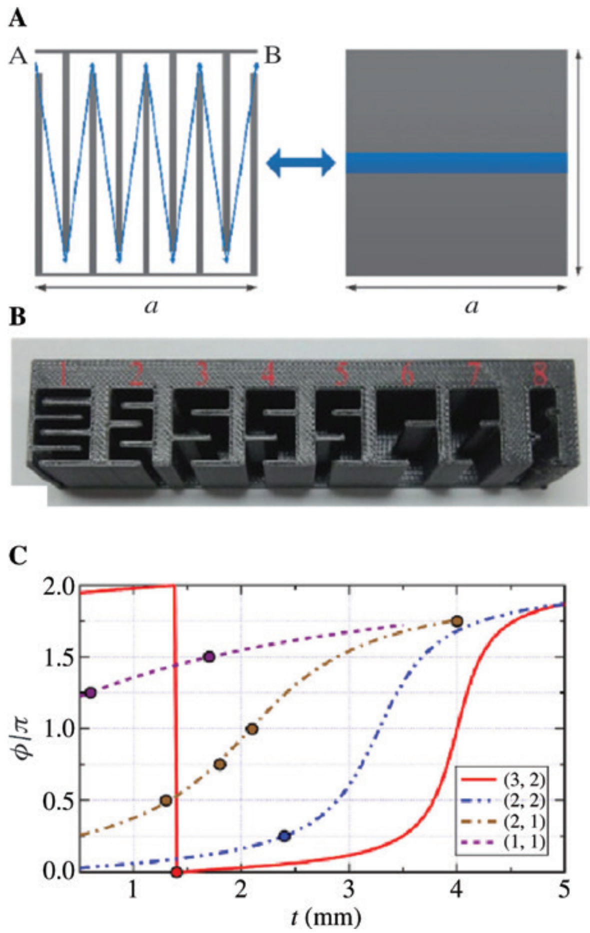

Figure 1: Reflective acoustic metasurface by coiling up space. (A) Schematic of space-coiling metamaterial units (left part) for mimicking a homogeneous effective medium with high refractive index. (B) Experimental sample of reflective-type acoustic metasurface (photo). (C) Simulated phase shift of metasurface units with different structural parameters (reprinted from Ref. [34]).

acoustic wave will be guided along the path marked by blue arrows after entering from the port near point A and eventually leave the system from port B, corresponding to a substantial elongation in the propagation distance without any change in the physical distance. Hence, such a labyrinthine-like air channel is equivalent to a straight channel filled with an effective medium of high refractive index (or low sound speed). Li et al. [34, 37] proposed the first theoretical model of acoustic metasurface for controlling reflected wavefront and then experimentally demonstrated a practical implementation (the photo of an experimental sample fabricated via 3D printing technique is shown in Figure 1B).

The proposed reflective-type acoustic metasurface is composed of an array of space-coiling type metamaterials with a closed end for reflecting all the incident acoustic energy back to the input port with an additional phase delay of $\varphi = kL$ (k is the wave number in air and L is the propagation distance). This suggests that the phase shift of the reflected wave on the acoustic metasurface can be tailored by adjusting the total length of the coiled channel. Typical numerical results are depicted in Figure 1C, which shows the phase shifts of the reflected wave generated by an individual unit cell for different combinations of structural parameters at a particular driving frequency of 3430 Hz. It can be observed that by adjusting a single parameter of the thickness of each plate used for sealing the zigzag channel in such space-coiling structure, the reflected phase can vary smoothly within the full range of $(0, 2\pi)$, which ensures the capability of shaping the wavefront for the incident acoustic wave illuminating the designed reflective-type metasurface. In Figure 1C, the (m, n) case means that there are m and n identical plates in the upper and lower boundaries in each unit cell, respectively, and the eight dots mark the phase shifts of the eight unit cells in Figure 1B (numbered as 1–8) which are chosen to cover a 2π range with a step of $\pi/4$. Notice that the equivalent propagation distance can be further enlarged by increasing the values of m and n (viz., increasing the total length of zigzag channel by using more identical plates in the labyrinthine structure), which however, also reduces the width of the air channel and necessarily leads to more severe viscosity loss. Hence, in the experimental demonstrations, less zigzagged structures are employed for minimizing loss of energy, as well as facilitating the sample fabrication.

The eight unit cells serve as the basic building blocks of reflective-type acoustic metasurfaces. The principle for designing acoustic metasurface can then be divided into two steps: (1) Derive the desired spatial distribution of phase shift required for producing the target wavefront-engineering phenomenon. For instance, for the purpose of designing a metasurface-based lens with planar surface and ultrathin thickness that can yield a focal spot located at $(f_x, 0) = (0.3\text{ m}, 0\text{ m})$, the equiphase surface should be the gray line shown in Figure 2A, and one can readily derive the phase profile that needs to be produced on the surface of acoustic metasurface:

$$\phi(y) = -k_0(\sqrt{y^2 + f_x^2} - x),$$

which is depicted in Figure 2B. (2) Based on the derived spatial phase distribution, discretize the continuous phase profile according to the dimension of basic building blocks and use a monolayer array of space-coiling metamaterial units, each of which is appropriately chosen from the eight units shown in Figure 1B to produce the required discrete

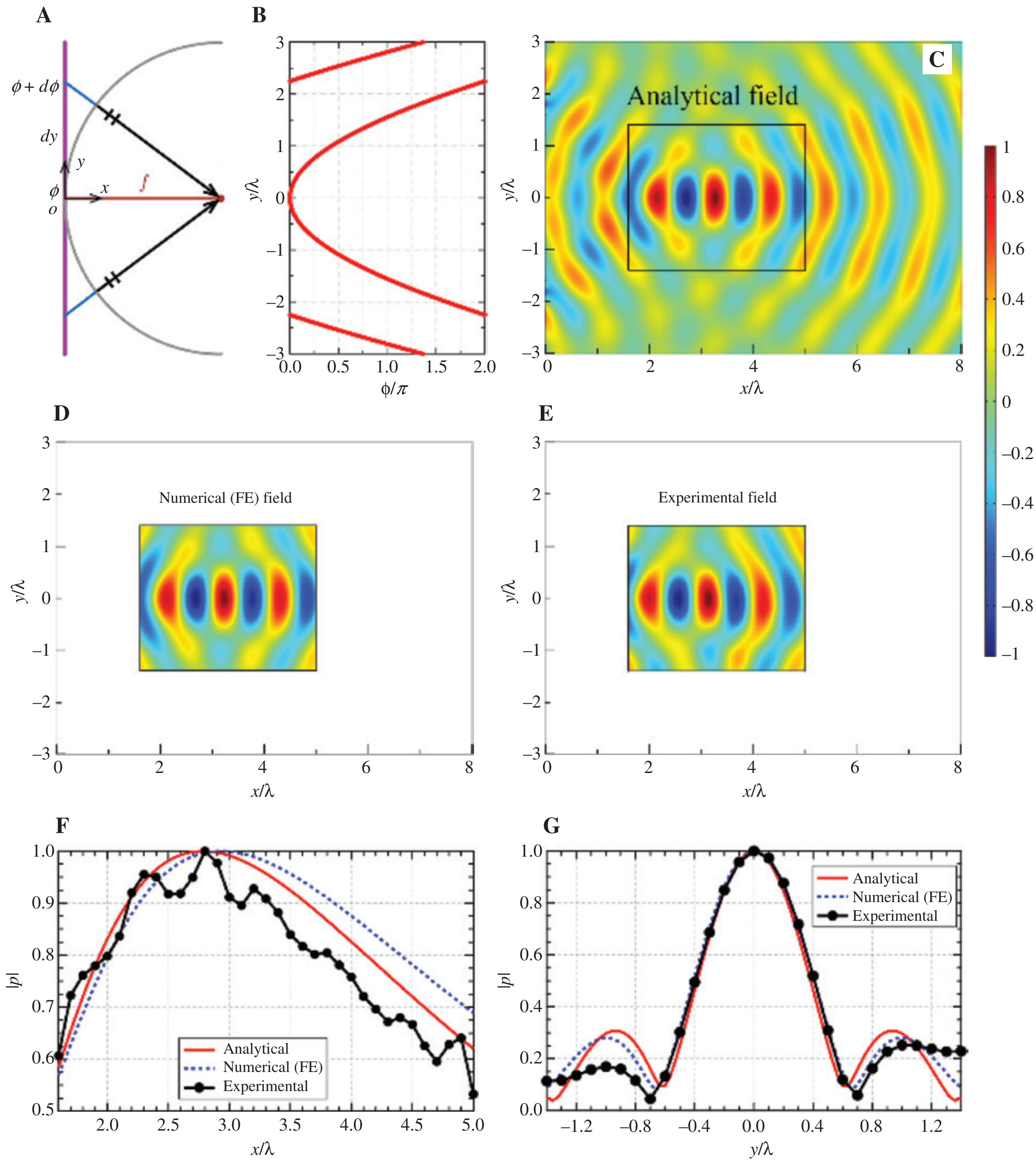

Figure 2: A planar and ultrathin lens for acoustic focusing.
(A) Schematic for deriving acoustic focusing by a planar and ultrathin lens. (B) The desired phase profile on the metasurfaces. (C) The pressure-field distribution predicted by Green's function theory with the black box indicating the region within which the measurement is performed. (D) The numerical simulation of metasurface composed by labyrinthine units and (E) the experimental results of the pressure-field distribution in the scanned region. (F, G) Acoustic pressure amplitude profiles (F) along the acoustic axis and (G) the radial direction in the focal plane (reprinted from Ref. [37]).

phase at y, to compose the acoustic metasurface capable of manipulating the reflected wavefront as desired.

Figure 2C–E plot, respectively, the spatial distribution of acoustic pressure predicted theoretically by Green's function theory (with the measured region being marked by the black box) and the numerical and experimental results of the pressure distribution in the measured region. The good agreement between these results clearly prove the capability of the designed acoustic metasurface to focus the incident acoustic energy into the predesigned spot despite its ultrathin thickness (~$\lambda_0/8$) and planar profile, which is also quantitatively evaluated via the comparison between the simulated and measured results of acoustic pressure amplitude profiles along the acoustic axis and the radial direction in the focal plane shown in Figure 2F and G.

By resorting to the specific acoustic impedance inhomogeneity and discontinuity which is one of the acoustic properties easy to control in reality, Zhao et al. [38] designed a planar surface with the special functionality of generating double reflections: the ordinary reflection and the extraordinary one whose wavefront is manipulated by the generalized Snell's law of reflection, and propose a scheme for realizing the complex discontinuity of the impedance surface using Helmholtz resonators. Particularly, it is proven that by adjusting the designed specific acoustic impedance, one can manipulate the extraordinary reflection while switching "on" or "off" the ordinary reflection (Figure 3). Later they propose an acoustic flat metasurface for controlling the vibrational orientations of fluid particles and demonstrate a complete conversion between two perpendicular vibrations by deviating the extraordinary reflection out of the incident plane. By using an array of straight tubes with properly designed lengths for implementing the designed scheme, they numerically show the out-of-incident-plane fluid-particle vibration and the arbitrary degree of freedom in directional manipulation along a 3D spatial angle.

Acoustic metasurfaces offer the possibility to manipulate reflected wavefront in ways unattainable in the nature, but their working bandwidths are inevitably limited due to the fact that the resonant subunits only produce the desired phase response at the designed frequency; moreover, the transverse size of a supercell needs to be related to wavelength; the change of frequency will unavoidably lead to different phase profiles. For tackling the problem of limited working bandwidth, Zhu et al. [39] proposed a scheme for designing a reflective metasurface capable of arbitrarily controlling the wavefront of reflected wave generated by it without bandwidth limitation. Based on strict analytical analysis, they predict thepossibility to eliminate frequency dependence with a specific spatial gradient of phase shift, as schematically shown in Figure 4A. A practical implementation of their design is demonstrated both numerically and experimentally by designing an array comprising subwavelength corrugated unit cells whose depths are properly tuned according to the theoretical predictions, via distinct phenomena of extraordinary acoustic reflection (Figure 4B and C) and generations of planar focusing and non-diffractive beam within an ultra-broad band. The physics mechanism underlying this design is elucidated by developing a simple physical model which predicts the upper cutoff frequency precisely. Bearing the advantages of nearly dispersion-free wave-steering capability

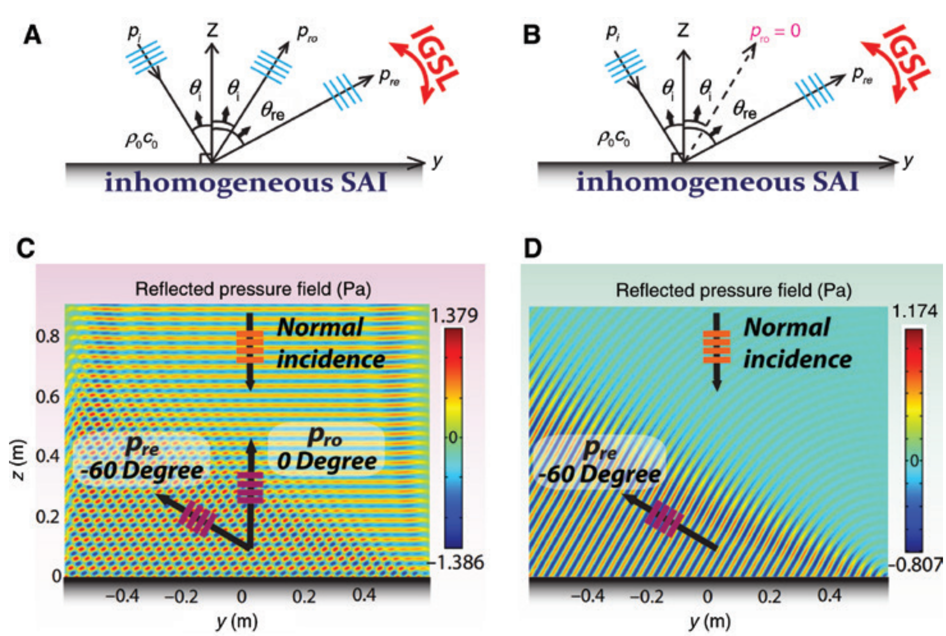

Figure 3: A flat interface with an inhomogeneous specific acoustic impedance for controlling reflection.
(A) Schematic of generation of ordinary and extraordinary reflections by a flat interface with an inhomogeneous specific acoustic impedance. (B) Suppression of ordinary reflection as the acoustic impedance is properly chosen. (C, D) Numerical results of the reflected pressure fields corresponding to cases (A) and (B) (reprinted from Ref. [38]).

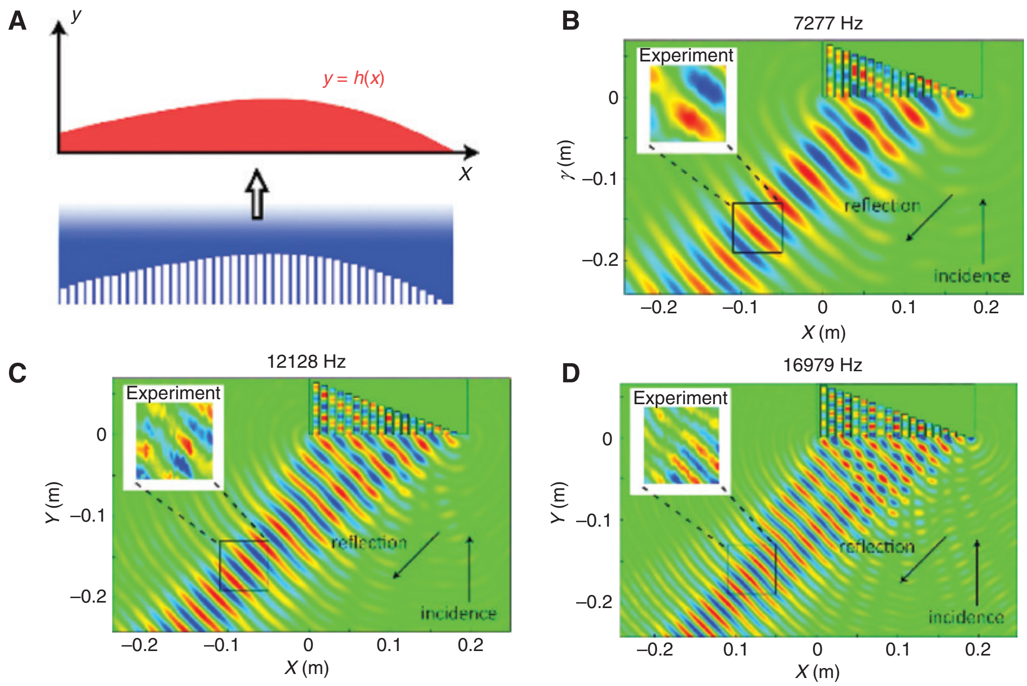

Figure 4: Reflective metasurfaces with nearly dispersion-free functionality.
(A) Schematic of metasurface made of grooves with subwavelength width below the surface. Blue region is filled with acoustically rigid medium, and the depth of grooves is a function of *x*. (B–D) Simulated and measured spatial distribution of extraordinary reflection at three particular frequencies (reprinted from Ref. [39]).

and deep discrete resolution, such a scheme may open a new avenue to the design and application of broadband acoustic devices.

4 Transmission-type acoustic metasurface

In the design of reflective-type acoustic metasurface, it is quite easy to ensure a high efficiency, since a nearly perfect total reflection of incident acoustic energy always occurs provided that a rigid boundary is used and the width of air channels is sufficiently large to avoid viscosity effect. When it comes to the manipulation of wavefront of transmitted acoustic wave, however, things become much different. A major difficulty lies in the fact that the transmission-type acoustic metasurfaces need not only to provide adjustable phase shift on the propagating wave but maintain a high transmission efficiency of acoustic energy. It is apparent that a low transmission coefficient means most of the acoustic energy is reflected back or absorbed when the incident wave traverses the designed metasurface, which will unavoidably diminish the effectiveness of the metasurface-based acoustic devices and limit their application potentials in practice.

Essentially, the condition for producing a high transmission efficiency for acoustic waves is to maintain the effective acoustical impedance, defined as the product of effective sound speed and effective mass density, matching the surrounding medium within which the acoustic metasurface is immersed. From the above discussion, the manipulation of propagating phase is inherently equivalent to the modulation of the effective sound speed (or effective refractive index) on acoustic metasurface. This means that only if the effective mass density and effective sound speed vary inversely can one achieve a high transmission efficiency and full control over the propagating phase simultaneously. Obviously, such a requirement is not attainable with naturally available materials, in which the acoustic waves propagate faster as the mass density becomes larger. For instance, the mass density and sound speed are 1.21 kg/m^3 and 343 m/s for air, 1000 kg/m^3 and 1500 m/s for water, and 7800 kg/m^3 and 6100 m/s for steel. By utilizing natural materials, it would become impossible to keep a constant acoustical impedance when varying the sound speed.

This seeming paradox can only be resolved by proposing acoustic metasurface units that provide unconventional acoustical properties with vanishing thicknesses. Li et al. [40] presented the theoretical design of a novel transmission-type metasurface composed of a monolayer array of subwavelength-scale elements comprising four Helmholtz resonators and a straight pipe (as schematically illustrated in Figure 5A), experimentally fabricated a 3D-printed sample (as shown in Figure 5B), and demonstrated its effectiveness. The width of an individual unit cell is $h=\lambda_0/10$, and the overall thickness of the resulting metasurface is $w=\lambda_0/2$.

The mechanism of such a design is that the series connection of four Helmholtz resonators is used to provide phase shift covering the full 2π range to the transmitted acoustic wave, while the introduction of straight pipe is for supporting hybrid resonance and compensating impedance mismatch between the metasurface element and the surrounding air. Thanks to the coupling between the Fabry-Perot resonance in the straight pipe and the four resonating Helmholtz cavities, a near-unity transmission efficiency persists as we modulate the propagating phase fully and smoothly by adjusting a single parameter of h_1, the height of straight pipe, as proved by the numerical results shown in Figure 5C (where the eight black dots mark the discrete phase shift provided by the eight unit cells employed in Figure 5B), in stark contrast to natural materials that cannot guarantee a tunable sound speed and matched acoustical impedance at the same time. Remarkably, the deep-subwavelength scale of such hybrid-structured unit, which can be 1 order of magnitude smaller than the working wavelength, helps to substantially improve the spatial resolution of phase profile, which is crucial for the production of high-quality and complicated acoustic field patterns.

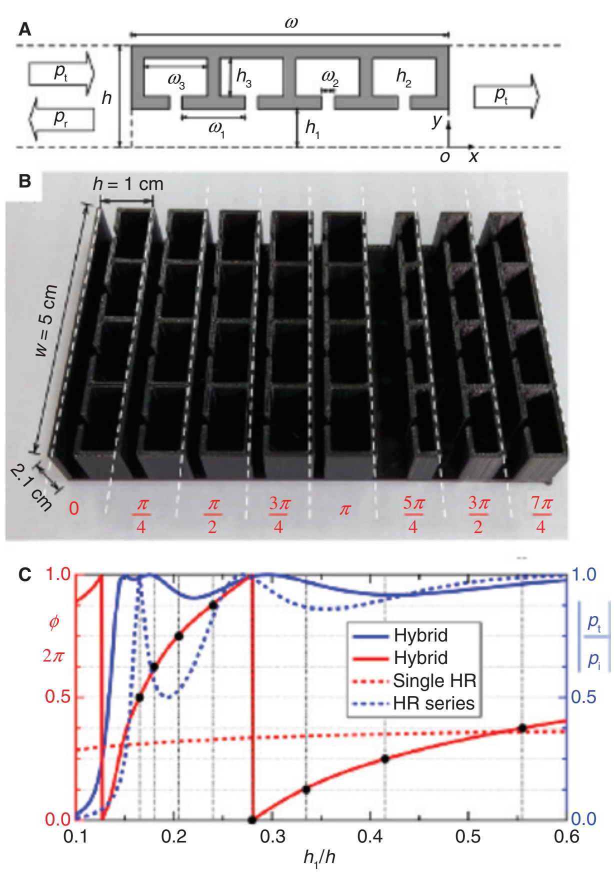

Figure 5: Design and implementation of transmission-type acoustic metasurface.
(A) Schematic of transmission-type acoustic metasurface with a hybrid structure comprising a straight pipe and four Helmholtz cavities. (B) Experimental sample (photo). (C) Phase shift (red, solid) and transmission rate (blue, solid) of the hybrid structureas a function of height ratio $h1=h$, and a comparison with that of Helmholtz resonators (red and blue dashed) (reprinted from Ref. [40]).

The advantages of such kind of acoustic metasurface in terms of reliability and spatial resolution was demonstrated by numerical simulations and experimental measurements, via the generation of self-bending beams beyond the paraxial approximation, which is challenging due to the rapidly varying phase shift along the metasurface. The ideal phase profile required for forming a self-bending beam in the nonparaxial approximation is depicted by the black line in Figure 6A. By discretizing this phase profile and choosing from the eight unit cells shown in Figure 5B, a transmission-type acoustic metasurface was built along the y direction. The numerical results shown in Figure 6B agree quite well with the measured data (Figure 6C), with both verifying that the cylindrical wave emitted from the source is modulated by the designed acoustic metasurface as desired, leading to a delivery of acoustic energy along the predesigned curved path after passing through the metasurface. A quantitative demonstration of the spatial distribution of sound pressure level in the propagation path is plotted in Figure 6C, which also shows a good agreement between the simulated and measured results and proves the effectiveness of the proposed metasurface in modulating the transmitted wavefront to form complex acoustic fields.

Besides the above-mentioned mechanism based on hybrid resonance, many other types of transmission-type acoustic metasurfaces were also designed for realizing versatile wavefront-steering functionalities for transmitted acoustic waves, such as by using the idea of coiling up space. Tang et al. [41] presented a design of metasurface structures that are made of spatially varied coiling-slit subunits and capable of serving as flat thin lens for anomalously deflecting the transmitted airborne sound. They proved numerically that by elaborately optimizing the geometries of subunits, the proposed scheme can produce high conversion efficiency over a broad range of frequencies and incident angles, which is verified by the experimental observation of redirected wavefronts agreeing well with theoretical predictions (Figure 7). Space-coiling-type

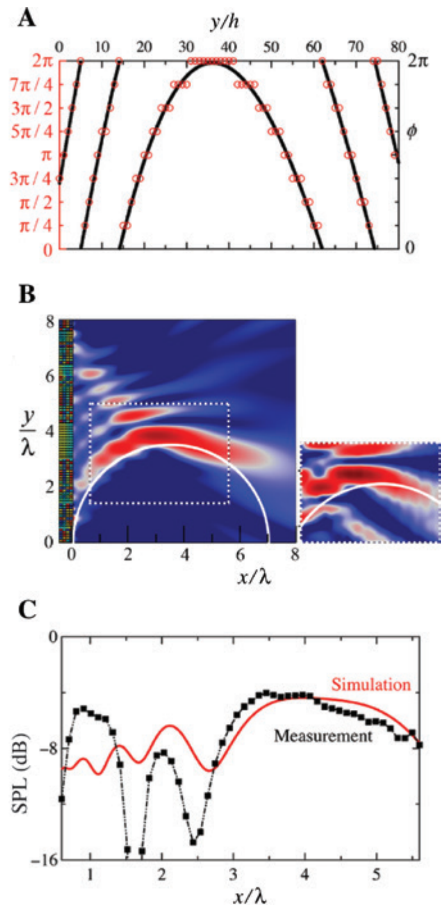

Figure 6: Production of self-bending beam based on acoustic metasurfaces.
(A) Phase profile required for generating self-bending beam (black line: ideal continuous curve, red circles: discrete phase shift produced by 80 elements along the screen). (B) Simulated and measured sound pressure level. White circle: thedesired sound path. White dotted rectangular region: scanning region in experiment. (C) Comparison of the simulated and measured results of the sound pressure level along the white-colored trajectory in (B) and (C) (reprinted from Ref. [40]).

metamaterials are also revised by Xie et al. [42] to have a taped labyrinthine configuration for producing different kinds of extraordinary wavefront engineering effects such as converting the propagating mode to evanescent surface mode and negative refraction (Figure 8). Recently, a novel helical-structured metamaterial was designed and experimentally realized by Zhu et al. [43] for providing a dispersive-free high effective refractive index (Figure 9), based on a substantial reduction in the group velocity due to the wavefront revolution in the designed compact structures. By adjusting the helicity, the slowness of the acoustic wave propagation can be freely tuned. A thin metasurface was constructed by arranging different helical structure units with properly designed helicities to experimentally act as a beam shaper capable of transforming a normal incidence plane wave into a self-accelerating beam on the prescribed parabolic trajectory.

A special kind of wavefront is the so-called acoustic vortices that have spiral phase dislocations and carry orbital angular momentum, in comparison to the above-mentioned ones with only linear momentum. Acoustic vortices have a spiral phase $\exp(im\theta)$with the carried orbital angular momentum being discretized with the integer m (referred to as topological charge or order of the beam), and possess very useful properties such as the capability of transferring the angular momentum to matter to produce a torque that can rotate tiny objects contactlessly. However, conventional methods for generating acoustic vortices have to rely on phased spiral sources, which consist of an array of individually addressed transducers and need to be sophisticated and highly costly, or physically spiral sources with screw dislocated profiles that have to be bulky and unevenly shaped [44–47].

To address these issues, Jiang et al. [48] proposed a different scheme for generating acoustic beams with orbital angular momentum. Instead of relying on the θ dependence in either the phase of incident wave field (such as by using the active phased arrays) or the propagation distance (such as by using structures with screw profiles), this mechanism straightforwardly produce the desired spiral phase of the outgoing wave by manipulating the effective wave number k_{eff} to become θ dependent. A metasurface was designed to demonstrate the performance of the mechanism both theoretically and experimentally via the generation of a first-order airborne vortex beam that has a smooth spiral phase and a Bessel-like profile, as shown in Figure 10. In comparison with the traditional ways for introducing orbital angular momentum, the acoustic resonance-based production of orbital angular momentum bears the unique advantages of high efficiency, compact size, and planar profile. It can therefore be expected that the use of acoustic metasurface provides a new way to control the orbital angular momentum of acoustic waves and may have deep implications in various applications such as rotation of objects by utilizing the rotational torque generated by acoustic vortices as demonstrated by Ye et al. [49] both numerically and experimentally.

5 Applications of acoustic metasurfaces

Considering the key role played by the wavefront manipulation in the field of acoustics in general, it can

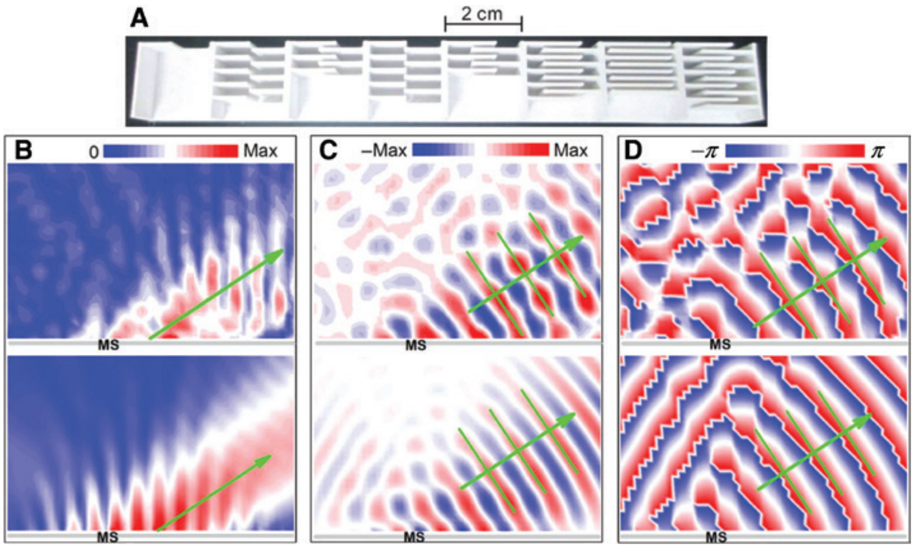

Figure 7: Transmission-type acoustic metasurfaces by coiling up spaces.
(A) Experimental sample (photo). (B–D) Measured (upper panels) and simulated (lower panels) amplitude, temporal, and phase field distributions, respectively. The green arrows indicate the propagating wavefronts predicted by generalized Snell's law (reprinted from Ref. [41]).

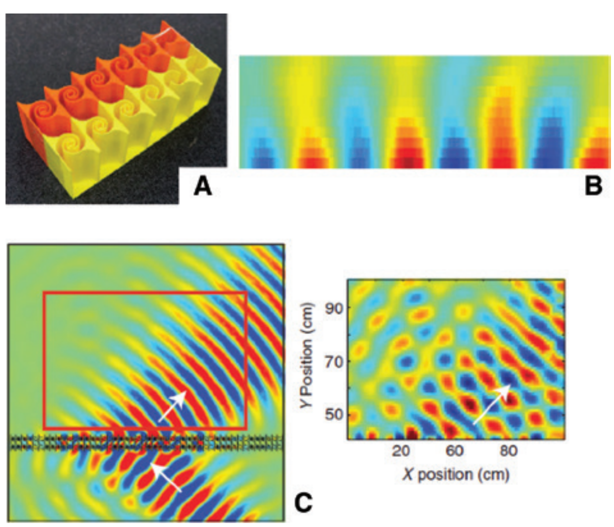

Figure 8: Acoustic metasurface based on taped labyrinthine structure.
(A) Fabricated taped labyrinthine unit cells (photo). (B) Measured near-field of the evanescent mode on the transmitted side for an incident angle of 25°. (C) Simulated and measured field pattern at 45° for demonstrating the negative refraction. The white arrows indicate the forward phase propagation directions (reprinted from Ref. [42]).

be expected that the recently emerged acoustic metasurfaces, as ultrathin and planar metamaterials with a reduced dimensionality, will open doors to a great variety of new promising applications and may even lead to revolutionary changes in acoustic techniques by breaking through the fundamental limits in conventional ones that have to rely on the use of natural materials. Indeed, the

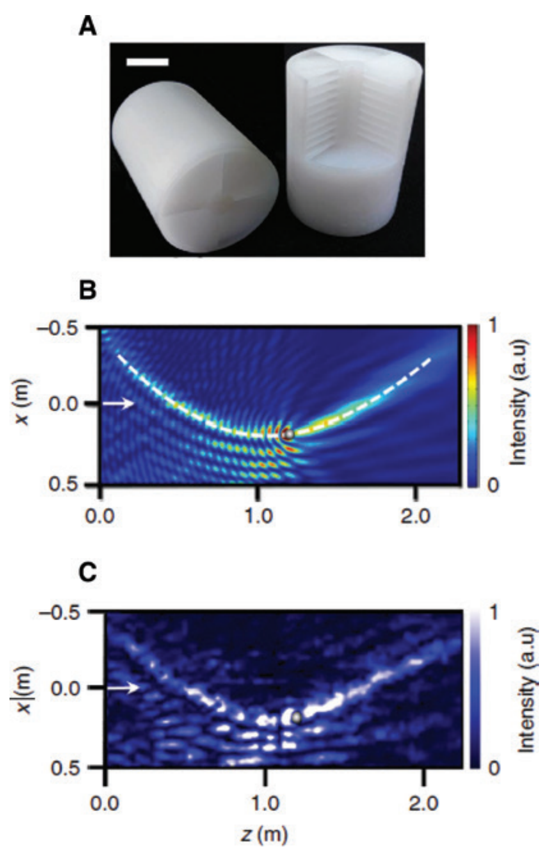

Figure 9: Helical-structured metasurface for generating self-accelerating beam.
(A) Fabricated helical-structured unit cell (photo). (B) The simulation demonstration of the self-healing properties of generated beam in which a rigid cylinder of diameter 4 cm is placed on the acoustic path. (C) The experimental results with the same-sized obstacle made of aluminum alloy (reprinted from Ref. [43]).

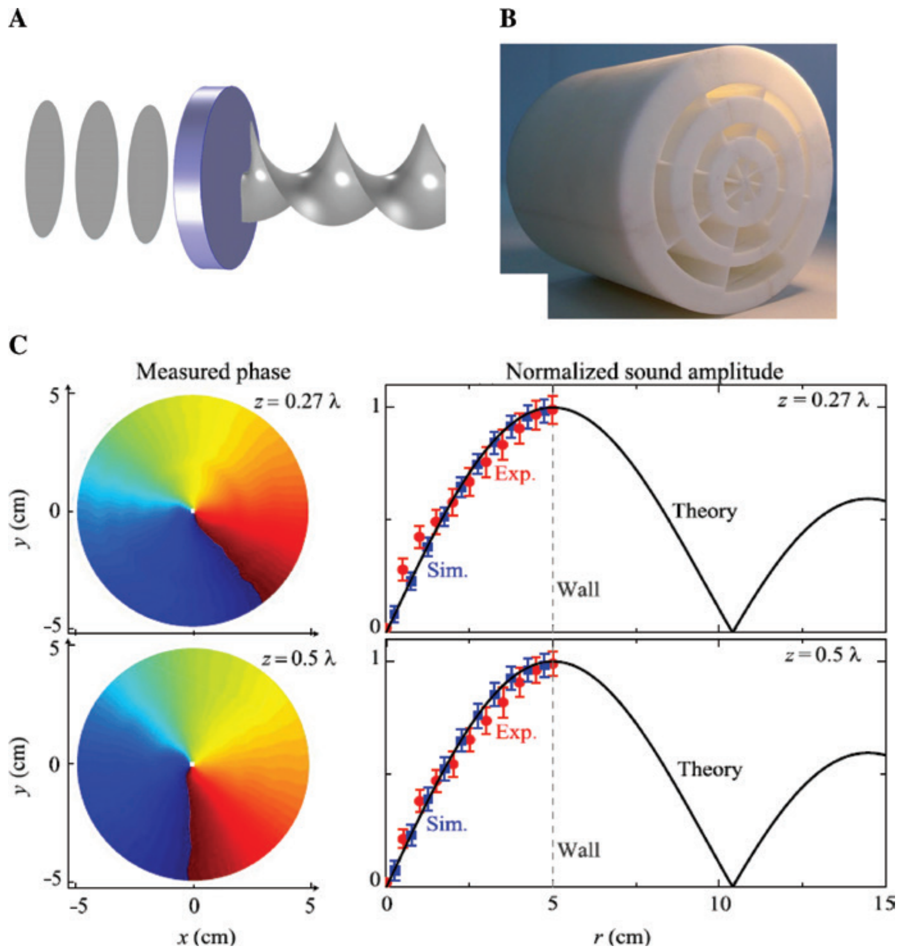

Figure 10: Metasurface-based conversion of acoustic resonance to orbital angular momentum.
(A) Schematic of the mechanism of converting acoustic resonance to orbital angular momentum. (B) Experimental sample (photo). (C) Simulated and measured results of the phase profile and sound amplitude on two different cross sections (reprinted from Ref. [48]).

latest couple of years have already witnessed many efforts dedicated to attempting to find practical applications of acoustic metasurfaces based on their unconventional functionalities of creating nearly arbitrary phase profile and controlling the wavefront of acoustic waves. This last section will review some representative advances in this aspect.

5.1 Metasurface-based acoustic diffusers

Acoustic diffusers are necessary for many places such as recording studios, concert venues, and movie theaters. The flat walls in a room always creates echoes and standing waves that may result in uneven sound quality. By placing sound diffusers on the walls and ceiling of a room, it is possible to scatter sound waves in all directions and thereby eliminate undesirable echoes and ultimately improve the quality of the sound. But the most commonly used Schroeder diffusers, proposed by Schroeder [50, 51] almost 50 years ago for artificially creating optimal and predictable sound diffuse reflection, have very bulky structures composed of an array of evenly spaced gratings that are identical in length and width but vary in depth. For generating diffuse reflection for incident acoustic waves, the Schroder diffusers need to produce a specific profile of phase shift on the surface such as a special number sequence. Conventionally, it is perceived that the phase of the acoustic wave can only be accumulated gradually along its propagation path, and the Schroeder diffusers are thus designed to produce the desired phase delay by controlling the sound path in a grating structure. In order to have a full range of phase shift covering a 2π range, the depth of individual units of grating, referred to as the “well,” can reach half of the wavelength of the lowest sound to be diffused (Figure 11A). This severely limits their applications in low-frequency range which, however, often covers the typical frequencies of many audible sounds such as voice. For example, a man’s voice as low as 85 Hz corresponds to a wavelength of 4 m, which

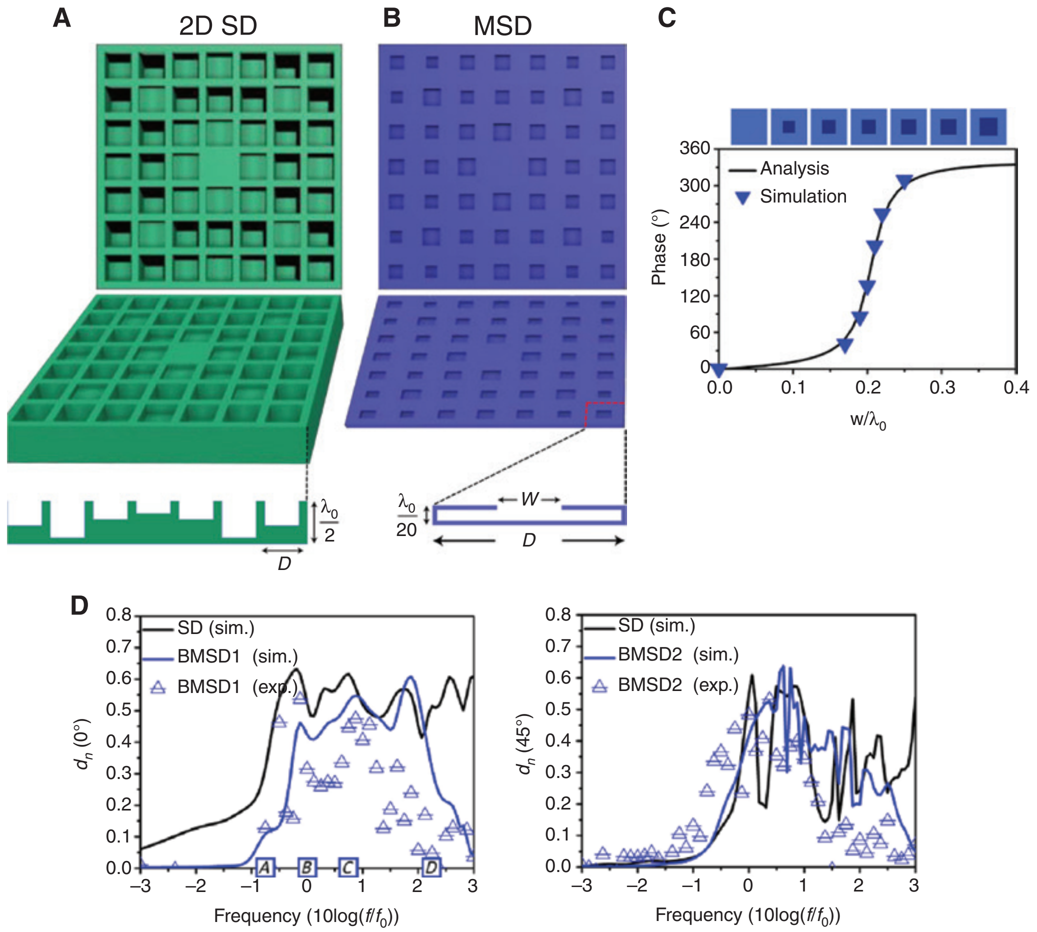

Figure 11: Comparison of traditional Schroeder diffusers and metasurface-based ultrathin Schroeder diffusers.
(A) Schematics of a 2D Schroeder diffuser and (B) the proposed metasurface-based Schroeder diffuser. (C) The analytical and simulated relationship between the phase shift and the geometrical parameter *w* at the center frequency of 6860 Hz. (D) Simulated and measured diffusion coefficient for 0° (left) and 45° (right) in the *x-z* plane versus frequency for broadband metasurface-based Schroeder diffuser and Schroeder diffuser, respectively (reprinted from Ref. [52]).

would need a Schroeder diffuser whose thickness reaches roughly 2 m.

Based on the concept of acoustic metasurfaces, Zhu et al. [52] have developed an "ultra-thin" sound diffuser 10 times thinner than the widely used conventional designs of Schroeder, as schematically illustrated in Figure 11B. For foresaid example of diffusing voice with a frequency of 85 Hz, the novel metasurface-based diffusers will only be 20 cm thick, which is quite applicable in practical situations. A 2D array of locally resonant elements, each of which is properly designed to produce a specific phase shift for the reflected waves, is arranged according to a specific quadratic residue sequence required by Schroeder's theory. By using Helmholtz-like resonators with ultrathin and planar profiles and wide necks, a wide phase change of 2π is achieved with such deep subwavelength unit cells (Figure 11C) while keeping the thermal and viscous losses, which are undesirable in the high-efficiency generation of sound diffuse reflection, much lower than the conventional Helmholtz resonators. An ultrathin version of Schroeder diffuser with a thickness of $\lambda_0=20$ has been demonstrated both numerically and experimentally. Indeed, this is also the thinnest acoustic metasurface that has been reported so far for manipulating the wavefront of transmitted or reflected waves with experimental verification (excluding those for absorption purposes, as will be reviewed in what follows).

Figure 11D plots the comparison between the simulated and measured diffusion coefficients of a conventional Schroeder diffuser and a broadband metasurface-based Schroeder diffuser that has a hybrid structure comprising components designed to generating the desired phase delay at different frequencies and therefore has broadened operating bandwidth, in which two incident angles (0° and 45°) are considered. The experiment results and simulation results are in reasonable agreement, showing that the proposed metasurface-based acoustic diffuser yields diffuse reflection at different frequencies, with high-efficiency performance on par with the widely commercialized Schroder diffusers. The new design uses less material and may result in lighter and cheaper diffusers that allow people to make better use of their space. This takes a major step towards applying acoustic metasurfaces to markedly improving conventional sound diffusers widely adopted in industry and solving practical acoustic problems, which may also provide a roadmap to wavefront manipulation and have far-reaching implications in architectural acoustics, noise control, and beyond [53].

5.2 Sound absorption by acoustic metasurfaces

It is of great interest, from both the scientific and engineering viewpoints, to realize a perfect absorber of deep-subwavelength scale which, however, remains challenging due to the aforementioned fundamental limitations in classic theory of acoustics. Conventional methods for absorbing acoustic energy include the use of porous materials, gradient index materials, or perforated panels, which usually lead to either imperfect match of acoustic impedance or very bulky structures whose sizes need to be comparable to the working wavelength [54]. Although acoustic absorbers can also be designed with active elements, the schemes of "active absorbers" necessarily result in high cost and sophisticated designs of electrical circuits. The existing designs of acoustic absorbers are not practical for low-frequency sound, calling for new mechanism to go beyond the fundamental barriers in traditional means and enable novel acoustic absorbers applicable in practice.

Ma et al. [55] proposed the idea of producing two resonances in deep-subwavelength layer with weak absorption and then placing the layer close to a rigid surface with a thin cell of sealed gas in between to hybrid these two resonances, as schematically shown in Figure 12A. With two useful degrees of freedom, such hybridized resonance helps to achieve robust impedance matching and perfect absorption. Figure 12B shows the frequency dependence of measured absorption coefficient for one unit cell of the proposed metasurface, manifesting the occurrence of a high and sharp absorption peak, which almost reaches unity, at 152 Hz as verified by the excellent agreement between the numerical and experimental results. The first eigenmode

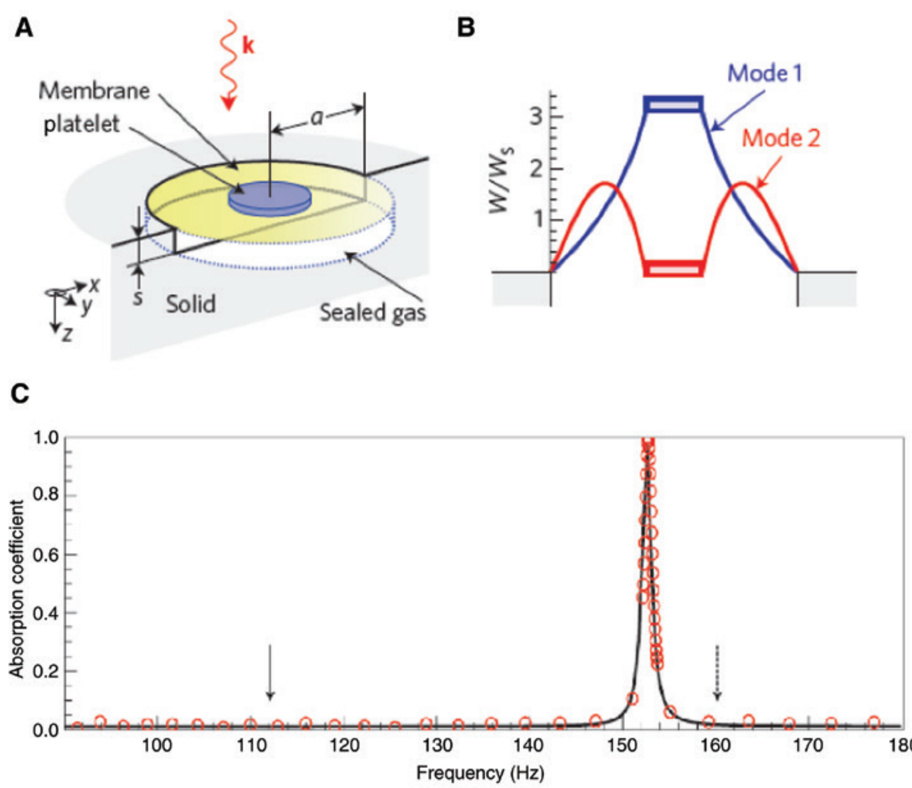

Figure 12: Acoustic metasurface with hybrid interfaces.
(A) Schematic illustration of the unit cell's components and geometry. (B) Schematic cross-sectional illustration of the two lowest frequency eigenmodes. (C) Measured absorption coefficient as a function of frequency. The solid and dashed arrows indicate the first eigenmode and anti-resonance (reprinted from Ref. [55]).

and anti-resonance are marked by the solid and dashed arrows, respectively. Interestingly, the absorption peak is located near the anti-resonance instead of at the eigenfrequency of the decorated membrane resonator, suggesting a novel absorption mechanism inherently different from the traditional ones that use only lossy materials.

To eliminate the dependence on prescribed tension of membrane that is inconvenient to adjust in practice, Li and Assouar [56] proposed the design of a metasurface-based absorber composed of a combination of a perforated plate and a coplanar air chamber with coiled configuration, for nearly totally absorbing the incident acoustic energy at an extremely low-frequency range around 125 Hz, as shown in Figure 13.

The viscosity in the perforated hole provides high absorption of incident acoustic energy at resonance but also leads to additional reactance and lowered impedance matching, which is compensated by the coplanar air chamber and realize matched impedance and perfect absorption as expected. Such a mechanism enables downscaling of the total thickness of the resulting device to as small as 1/223 of the operating wavelength, which is much thinner than the conventional designs as well as the abovementioned metamaterial-based absorbers. By solving the basic problem of absorbing low-frequency sound perfectly with deep subwavelength scale, the metasurface-based acoustic absorber takes advantage of compactness, planar profile, stable structure, and high efficiency and may pave the way towards the design of related functional devices and their applications in various important scenarios such as noise control and energy harvesting.

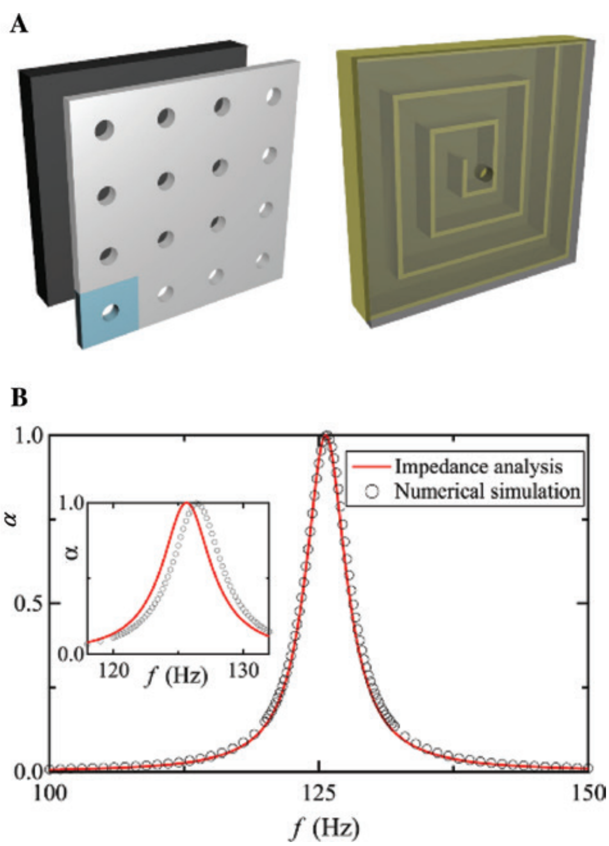

Figure 13: Metasurface-based absorber.
(A) Conventional perforated system with a perforated plate placing in front of a hard object. (B) The metasurface composed of a perforated plate with a hole and a coiled air chamber. (C) The absorption coefficient of the presented metasurface (black circles) with geometrical parameters (reprinted from Ref. [56]).

6 Summary

Since the first emergence of the concept of acoustic metasurfaces in 2013, this research field has undergone a rapid expansion during the past few years and attracted great attention from within and beyond the acoustics community. Because of the two-dimensional nature of the metasurface structures, they occupy less physical space and offer an alternative to bulk three-dimensional metamaterials for realizing versatile functionalities of steering wavefront almost arbitrarily, offering new general paradigm of artificial functional devices with great application prospects. Despite the advances in the new physics enabled by acoustic metasurfaces and the proposed metasurfaces-based devices that have preliminarily bridged the gap between real world applications, it is noteworthy that some important questions still remain largely unanswered, including the (i) mechanism for designing dispersionless acoustic metasurfaces that can go beyond the limitation of working bandwidth in the current resonance-based metasurfaces while maintaining the subwavelength nature, (ii) evolution of acoustic metasurfaces from linear to nonlinear regime to enable generating special nonlinear response at subwavelength scale, and (iii) development of non-Hermitian acoustic capable of making use of loss effect – which is unavoidable when downscaling the metamaterial units and traditionally thought harmful to wave manipulation – to open new degree of freedom for further extending the functionality of resulting devices, etc. It can be anticipated that in the future, by exploring novel mechanisms and gaining deeper insight into the unconventional wavefront-engineering functionality of acoustic metasurfaces, there will be further progresses on the integration and miniaturization of devices as well as energy efficiency that far surpass those of the bulk acoustic components widely used in conventional approaches, leading to revolutionary technological breakthroughs in acoustics and related areas.

References

[1] Smith DR, Pendry JB, Wiltshire MCK. Metamaterials and negative refractive index. Science 2004;305:788–92.

[2] Enoch S, Tayeb G, Sabouroux P, Guérin N, Vincent P. A metamaterial for directive emission. Phys Rev Lett 2002;89:213902.

[3] Smith DR, Vier DC, Koschny T, Soukoulis CM. Electromagnetic parameter retrieval from inhomogeneous metamaterials. Phys Rev E 2005;71:036617.

[4] Smith DR, Mock JJ, Starr AF, Schurig D. Gradient index metamaterials. Phys Rev E 2005;71:036609.

[5] Li J, Chan CT. Double-negative acoustic metamaterial. Phys Rev E 2004;70:055602.

[6] Fang N, Xi D, Xu J, et al. Ultrasonic metamaterials with negative modulus. Nat Mater 2006;5:452–6.

[7] Ding Y, Liu Z, Qiu C, Shi J. Metamaterial with simultaneously negative bulk modulus and mass density. Phys Rev Lett 2007;99:093904.

[8] Liu Z, Zhang X, Mao Y, et al. Locally resonant sonic materials. Science 2000;289:1734–6.

[9] Cummer SA, Christensen J, Alu A. Controlling sound with acoustic metamaterials. Nat Rev Mater 2016;1. Article no: 16001.

[10] Ma GC, Sheng P. Acoustic metamaterials: from local resonances to broad horizons. Sci Adv 2016;2:e1501595.

[11] Christensen J, García de Abajo F. Negative refraction and backward waves in layered acoustic metamaterials. Phys Rev B 2012;86. Article no: 024301.

[12] Liu F, Huang X, Chan CT. Dirac cones at $\vec{k}=0$ in acoustic crystals and zero refractive index acoustic materials. Appl Phys Lett 2012;100:071911.

[13] Jing Y, Xu J, Fang NX. Numerical study of a near-zero-index acoustic metamaterial. Phys Lett A 2012;376:2834–7.

[14] Li Y, Liang B, Gu ZM, Zou XY, Cheng JC. Unidirectional acoustic transmission through a prism with near-zero refractive index. Appl Phys Lett 2013;103:053505.

[15] Daniel T, José SD. Anisotropic mass density by two-dimensional acoustic metamaterials. New J Phys 2008;10:023004.

[16] Torrent D, Sánchez-Dehesa J. Radial wave crystals: radially periodic structures from anisotropic metamaterials for engineering acoustic or electromagnetic waves. Phys Rev Lett 2009;103:064301.

[17] Norris AN. Acoustic metafluids. J Acoust Soc Am 2009;125:839–49.

[18] Gu ZM, Liang B, Zou X, et al. One-way acoustic mirror based on anisotropic zero-index media. Appl Phys Lett 2015;107:213503.

[19] Gu ZM, Jiang X, Liang B, et al. Experimental realization of broadband acoustic omnidirectional absorber by homogeneous anisotropic metamaterials. J Appl Phys 2015;117:074502.

[20] Ma GC, Fu C, Wang G, et al. Polarization bandgaps and fluid-like elasticity in fully solid elastic metamaterials. Nat Commun 2016;7:13536.

[21] Zhang S, Yin L, Fang N. Focusing ultrasound with an acoustic metamaterial network. Phys Rev Lett 2009;102:194301.

[22] Li JS, Fok L, Yin XB, Bartal G, Zhang X. Experimental demonstration of an acoustic magnifying hyperlens. Nature Mater 2009;8:931–4.

[23] Li JS, Pendry JB. Hiding under the carpet: a new strategy for cloaking. Phys Rev Lett 2008;101:203901.

[24] Chen H, Chan CT. Acoustic cloaking and transformation acoustics. J Phys D Appl Phys 2010;43:113001.

[25] Zhu XF, Liang B, Kan WW, Zou XY, Cheng JC. Acoustic cloaking by a superlens with single-negative materials. Phys Rev Lett 2011;106:014301.

[26] Kan W, García-Chocano VM, Cervera F, Liang B, Zou X. Broadband acoustic cloaking within an arbitrary hard cavity. Phys Rev Appl 2015;3:064019.

[27] Kan W, Liang B, Zhu X, et al. Acoustic illusion near boundaries of arbitrary curved geometry. Sci Rep 2013;3:1427.

[28] Kan W, Liang B, Li R, et al. Three-dimensional broadband acoustic illusion cloak for sound-hard boundaries of curved geometry. Sci Rep 2016;6:36936.

[29] Yu N, Genevet P, Kats MA, et al. Light propagation with phase discontinuities: generalized laws of reflection and refraction. Science 2011;334:333–7.

[30] Holloway CL, Kuester EF, Gordon JA, O'Hara J, Booth J, Smith DR. An overview of the theory and applications of metasurfaces: the two-dimensional equivalents of metamaterials. IEEE Antenn Propag 2012;M54:10–35.

[31] Pors A, Nielsen MG, Eriksen RL, Bozhevolnyi SI. Broadband focusing flat mirrors based on plasmonic gradient metasurfaces. Nano Lett 2013;13:829–34.

[32] Huang LL, Chen X, Mühlenbernd H, et al. Three-dimensional optical holography using a plasmonic metasurface. Nature Commun.2013;4:2808.

[33] Huang LL, Chen X, Bai B, et al. Helicity dependent directional surface plasmon polariton excitation using a metasurface with interfacial phase discontinuity. Light-Sci Appl 2013;2:e70.

[34] Li Y, Liang B, Gu ZM, Zou XY, Cheng J.C. Reflected wavefront manipulation based on ultrathin planar acoustic metasurfaces. Sci Rep 2013;3:2546.

[35] Liang Z, Li J. Extreme acoustic metamaterial by coiling up space. Phys Rev Lett 2012;108:114301.

[36] Liang Z, Feng T, Lok S, et al. Space-coiling metamaterials with double negativity and conical dispersion. Sci Rep 2013;3:1614.

[37] Li Y, Jiang X, Li R, et al. Experimental realization of full control of reflected waves with subwavelength acoustic metasurfaces. Phys Rev Appl 2014;2:064002.

[38] Zhao JJ, Li BW, Chen ZN, Qiu CW. Manipulating acoustic wavefront by inhomogeneous impedance and steerable extraordinary reflection. Sci Rep 2013;3:2537.

[39] Zhu Y-F, Zou X, Li R, et al. Dispersionless manipulation of reflected acoustic wavefront by subwavelength corrugated surface. Sci Rep 2015;5:10966.

[40] Li Y, Jiang X, Liang B, Cheng J-C, Zhang L. Metascreen-based acoustic passive phased array. Phys Rev Appl 2015;4:024003.

[41] Tang K,, Qiu C, Ke M, Lu J, Ye Y, Liu Z. Anomalous refraction of airborne sound through ultrathin metasurfaces. Sci Rep 2014;4:6517.

[42] Xie YB, Wang W, Chen H, Konneker A, Popa B-I, Cummer SA. Wavefront modulation and subwavelength diffractive acoustics with an acoustic metasurface. Nature Commun 2014;5:5553.

[43] Zhu XF, Li K, Zhang P, et al. Implementation of dispersion-free slow acoustic wave propagation and phase engineering with helical-structured metamaterials. Nature Commun 2016;7:11731.

[44] Marchiano R, Thomas JL. Synthesis and analysis of linear and nonlinear acoustical vortices. Phys Rev E 2005;71:066616.

[45] Baresch D, Thomas JL, Marchiano R. Observation of a single-beam gradient force acoustical trap for elastic particles: acoustical tweezers. Phys Rev Lett 2016;116:024301.
[46] Riaud A, Thomas J-L, Charron E, Bussonnière A, Matar OB, Baudoin M. Anisotropic swirling surface acoustic waves from inverse filtering for on-chip generation of acoustic vortices. Phys Rev Appl 2015;4:034004.
[47] Jiang X, Zhao J, Liu S, et al. Broadband and stable acoustic vortex emitter with multi-arm coiling slits. Appl Phys Lett 2016;108:203501.
[48] Jiang X, Li Y, Liang B, Cheng J-C, Zhang L. Convert acoustic resonances to orbital angular momentum. Phys Rev Lett 2016;117:034301.
[49] Ye LP, Qiu C, Lu J, et al. Making sound vortices by metasurfaces. AIP Adv 2016;6:085007.
[50] Schroeder MR. Diffuse sound reflection by maximum-length sequences. J Acoust Soc Am 1975;57:149–50.
[51] Schroeder MR. Binaural dissimilarity and optimum ceilings for concert halls – more lateral sound diffusion. J Acoust Soc Am 1979;65:958–63.
[52] Zhu Y, Fan X, Liang B, Cheng J, Jing Y. Ultrathin acoustic metasurface-based schroeder diffuser. Phys Rev X 2017;7:021034.
[53] Fan XD, Zhu Y-F, Liang B, Yang J, Yang J, Cheng J-C. Ultra-broadband and planar sound diffuser with high uniformity of reflected intensity. Appl Phys Lett 2017;111:103502.
[54] Jiang X, Liang B, Li R, Zou X, Yin L, Cheng JC. Ultra-broadband absorption by acoustic metamaterials. Appl Phys Lett 2014;105:243505.
[55] Ma GC, Yang M, Xiao SW, Yang ZY, Sheng P. Acoustic metasurface with hybrid resonances. Nature Mater 2014;13:873–8.
[56] Li Y, Assouar BM. Acoustic metasurface-based perfect absorber with deep subwavelength thickness. Appl Phys Lett 2016;108:063502.